7-1-1994

Fracture Toughness of Electrogas Welds in Double-Hull Construction

Eric J. Kaufmann

Peiyuan Xu

Mark R. Kaczinski

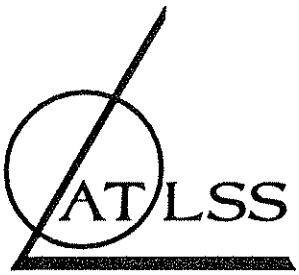

ADVANCED TECHNOLOGY FOR
LARGE
STRUCTURAL SYSTEMS

Lehigh University

Fracture Toughness of Electrogas Welds In Double-Hull Construction

by

Eric J. Kaufmann
Research Engineer

Peiyuan Xu
Research Associate

Mark R. Kaczinski
Research Engineer

ATLSS Report No. 94-08

July 1994

ATLSS Engineering Research Center
Lehigh University
117 ATLSS Dr., Imbt Laboratories
Bethlehem, PA 18015-4729
(610) 758-3525

An NSF Sponsored Engineering Research Center

ABSTRACT

A new tanker design currently under development incorporates new design and fabrication features which are expected to reduce shipbuilding costs by as much as 30 percent and provide for environmentally safe transport of oil products. This new double-hull design incorporates 2.1 m x 2.4 m x 15.2 m (7'x8'x50') cellular modules joined into 172-268 metric ton (190-295 ton) hull sub-assemblies. The sub-assemblies can be incorporated into new or existing single-hulled ships. As currently planned, the two hull plates and cell web girder of each module will be joined with a single, continuous weld pass in a vertical orientation using the Electrogas welding (EGW) process. The EGW process was selected because of the high deposition rates which can be achieved (23 kg/hr) and corresponding high productivity.

Because of uncertainties associated with the weld process stemming from experiences with the related electroslag welding (ESW) process regarding fatigue and low fracture toughness, studies were undertaken to evaluate the fatigue and fracture behavior of this weld detail. The results of the fatigue study were reported previously. The current study is a follow-on which examines the fracture toughness of the electrogas weld metal. Elastic-plastic fracture toughness (J_{IC}) and Charpy V-notch (CVN) impact toughness tests were performed on a test plate fabricated using the same materials and weld procedures as used in full-size fabrications. Compact tension (CT) and Charpy V-notch test specimens were fabricated from the weld metal in the L-T and T-L orientation. Additional test specimens were located in the heat-affected-zone (HAZ) and base plate (ABS Grade CS). A total of 12 compact tension specimens and 72 CVN specimens were tested.

Test results from both compact tension and CVN tests indicated that the fracture toughness of the base metal, weld metal and HAZ were similar. The CVN tests indicated a 20 J (15 ft-lb) transition temperature of at least -40 C. The J_{IC} tests performed in accordance with ASTM E 813 resulted in J_{IC} values in the weld metal and HAZ ranging from 106-146 kJ/m^2 (608-834 $in\text{-}lb/in^2$) which correlate to K_C values of 148-174 $MPa(m)^{1/2}$ (135-158 $ksi(in)^{1/2}$). No significant orientation effect was observed in the weld metal. Based upon the types and sizes of fabrication flaws observed in the previous fatigue study, an assessment of their fracture sensitivity was performed in light of the measured fracture toughness. It was concluded that none of the observed fabrication flaws were critical from a fracture viewpoint and that critical flaw sizes were through-thickness and large enough to be detected by visual inspection.

TABLE OF CONTENTS

1. INTRODUCTION

An experimental study recently completed at the ATLSS Center at Lehigh University evaluated the fatigue resistance of longitudinal electrogas welds (EGW) used to join the web and top flange of large scale beam specimens [1]. The specimens were fabricated to simulate the weld detail used to join hull plates on the Marc Guardian double-hull tanker under development by Marinex International Inc. and Metro Machine Corp. This new tanker design incorporates 2.1 m × 2.4 m × 15.2 m (7'x8'x50') cellular modules consisting of both inner and outer hull plates which are curved to add strength and stability to the double-hull section. Current plans are for the 15.2 m (50 ft) long modules to be fabricated in a vertical orientation which allows the two curved hull plates and cell web to be joined with a single, continuous electrogas weld pass. The results of this study indicated that a conservative lower-bound estimate for the fatigue strength of longitudinal electrogas welds is the AASHTO [2] category B' S/N curve. All fatigue failures, including those caused by significant weld metal porosity or cold cracks, were above the category B' curve.

Because of the high heat inputs associated with the EGW process and past experiences of poor fracture toughness in welds fabricated with the related electroslag (ESW) process, a pilot study was also conducted on the mechanical properties of the welded joint. Although this pilot study indicated an acceptable level of notch toughness and ductility, it was suggested that a more comprehensive research program be conducted on this topic. Therefore, the primary objective of the present research program was to better define the fracture toughness properties of longitudinal electrogas welds fabricated using conditions and weld parameters identical to those to be used in construction of the Marc Guardian double-hull tanker. The ATLSS Center at Lehigh University was contracted by Metro Machine Corporation to obtain experimental data on the fracture toughness of the electrogas weld metal and to also utilize this information to perform an assessment of fracture critical flaw sizes which could be anticipated in the weld metal.

Elastic-plastic fracture toughness (J_{IC}) and Charpy V-notch toughness test results were obtained from tests of compact tension (CT) specimens tested in accordance with ASTM E813 and standard Charpy V-notch (CVN) specimens both tested from three locations and/or orientations within the EGW detail. The weld metal test specimens were machined both transverse and longitudinal to the weld axis and longitudinal to the weld axis for the heat-affected-zone (HAZ) of the base plate. Tests were also performed on the unaffected base plate for comparison. An estimate of fracture critical flaw sizes was conducted using linear elastic

fracture mechanics. Estimates were performed on weld details with fabrication flaw sizes and locations representative of those observed in the fatigue testing program.

2. FRACTURE TOUGHNESS TEST PROGRAM

2.1 Materials and Test Specimens

Test specimens were machined from a 2590 mm (8.5 ft) long by 327 mm (12.88 in) wide welded panel fabricated by Metro Machine Corporation in Norfolk, VA. The panel contained a full-length, longitudinal hull seam weld made with the electrogas welding process. This full penetration square groove weld joins two flange plates and a simulated web plate in a continuous single pass as illustrated in Figure 1. An etched cross-section of the weld is shown in Figure 2.

Material properties, and thickness, of the flange and web plates used in the test panel simulate what is specified for the prototype tanker design, although the joint geometry has been slightly modified to not include the 104 degree flared top flange configuration for convenience in test specimen fabrication. A 25 mm (1 in.) thick, normalized, low carbon steel plate meeting American Bureau of Shipping (ABS) Grade AB/CS specifications was used for the flanges and a 25 mm (1 in.) thick, low carbon steel plate meeting ABS Grade AB/A specifications was used for the web. Both materials have a specified minimum yield strength of 234 MPa (34 ksi).

The EGW panel was fabricated vertically in a 15.2 m (50 ft) high tower which was built exclusively for the Marc Guardian project. A mechanized, movable platform on the tower contains the necessary welding equipment and tracks the water-cooled copper shoe along the front face of the EGW. The joint was completed following all appropriate ASNI/AWS specifications [3,4] using an AWS EG-82T-G self-shielding flux-cored electrode. Prior to shipping the test panel, the weld was inspected visually and ultrasonically by Metro Machine Corporation. Two weld defects were identified in the test panel during the ultrasonic inspection. These areas were avoided in laying out the test specimens.

Sets of 3 compact tension and 18 Charpy V-notch (CVN) impact toughness test specimens were machined within the electrogas weld metal, the heat-affected-zone (HAZ), and base metal as shown in Figure 3. The three Type "A" compact tension and 18 Type "A" Charpy V-notch specimens were machined from the weld material in the transverse-longitudinal (T-L) orientation

with the notch placed in the direction of welding. CVN specimens were removed from the mid-thickness location of the weld. Standard CT specimens were fabricated as close to full plate thickness as possible. The dimensions of the CT specimen are shown in Figure 4. An additional set of specimens, designated as Type "C", were fabricated from the weld metal in the longitudinal-transverse (L-T) orientation. The tip of the machined notch in the Type "C" compact tension specimens was positioned at the EGW fusion line and fatigue precracked into the weld metal. Compact tension and CVN specimens were also machined in the T-L orientation with the machined notch positioned within the coarse grained HAZ (Type "B"). The surface of the specimens were chemically etched prior to notching to locate the fusion line and then notched 0.25-0.50 mm beyond the fusion line. Finally, a set of Type "D" specimens were also machined in the T-L orientation of the flange plate adjacent to the location of Type "B" HAZ specimens.

2.2 Test Procedure

2.2.1 Charpy V-Notch Tests

The four sets of 18 test specimens corresponding to L-T and T-L orientations of weld metal, T-L oriented base metal, and T-L oriented HAZ specimens were tested in triplicate at several test temperatures in the transition temperature range. The test method used was in accordance with ASTM E-23.

2.2.2 J_{IC} Fracture Toughness Tests

Fracture toughness tests were performed using the test method prescribed in ASTM E-813-89 [5]. The single specimen unloading compliance technique was used permitting development of an entire J-R curve from a single CT specimen. Testing was carried out using a PC controlled closed loop servohydraulic test machine and commercially available software (Fracture Technology Associates) for elastic-plastic fracture toughness testing and analysis.

Dimensions of the twelve specimens tested are given in Table 1. Three Type D specimens were prepared and tested however it was discovered after testing specimen D2 that the fatigue precrack did not satisfy crack straightness requirements of the test specification and was discarded. After fatigue precracking all of the test specimens and testing the first specimen (D1), it was noted that the crack extension which developed had tunnelled considerably in the

interior of the specimen resulting in unacceptable unevenness in the crack shape. This results in errors in determination of the crack length by the compliance method and consequently errors in determining Δa. It was decided to modify the remaining specimens by introducing side grooves on the specimen sides (see Figure 4) to aid in maintaining a uniform crack extension across the entire crack front. This is an effective and accepted technique for reducing crack tunneling and does not appreciably change the specimen thickness.

All tests were carried out at room temperature (approximately 20 C). After testing, specimens were heat tinted in an oven to mark the final crack length prior to fracturing the specimen at liquid nitrogen temperature. Initial and final crack length measurements were obtained and checked with the compliance calculated crack lengths. Calculations in the J-R curve development were performed using the same commercial sofware as was used in the testing. Flow stresses, σ_f, for the base metal, HAZ, and weld metal were estimated as 379 MPa (55 ksi), 430 MPa (62.5 ksi), and 482 MPa (70 ksi) respectively.

3. TEST RESULTS

3.1 Charpy V-Notch Tests

The results of the base metal, weld metal, and HAZ Charpy V-notch tests are tabulated in Table 2. Figure 5 shows a plot of the base metal results along with results obtained for the heat of ABS Grade CS steel used in the fatigue testing program [1]. These are included to provide at least some indication of the variability in toughness which can be expected in this material. The plate used in the present study has a lower upper shelf toughness however the transition temperature range of the two are very nearly the same. The 20 J (15 ft-lb) transition temperature for both plates is between -40 and -60 C.

Figure 6 shows a plot of the weld metal test results for the T-L oriented (Type A) and L-T oriented (Type C) test specimens. Despite the large difference in grain structure in the two orientations, the notch toughness appears to be nearly identical. The 20 J (15 ft-lb) transition temperature in both cases is between -60 and -80 C.

The results of the HAZ tests are shown in Figure 7 in relationship to the base metal and weld metal test results. A reduction in toughness compared to the unaffected base metal is

evident however the transition temperature has not shifted appreciably. The 20 J transition temperature remains about -40 C.

Viewing the test results in Figure 7 collectively indicates that the notch toughness of the weld joint, composed of unaffected base metal, heat affected base metal, and weld metal, is very nearly the same. Viewed from a transition temperature approach to fracture, fracture would not be expected to occur in these materials under plane strain conditions for static or impact loading at service temperatures above -40 C. Fracture above this temperature can be expected to be elastic-plastic or fully plastic depending upon the temperature and loading rate.

3.2 J_{IC} Fracture Toughness Tests

Figures 8 through 12 show representative load vs. displacement and corresponding J-Δa plots for each of the four types of CT test specimens. A summary of the results for all CT tests is given in Table 3. Nearly all requirements for test validity were met in the CT tests. Specimen thickness requirements (ie. $B > 25\ J_Q/\sigma_y$) were satisfied. Small deviations in crack extension straightness which exceeded the E813 requirements were measured, however, and therefore the results are reported in Table 3 as J_Q values. This is expected to have only a small influence on the calculated toughness. A J_C-K_C correlation frequently used is also given in the table. Previous tests [6] on several steels with a range of yield strengths, including ABS Grade B steel, have shown this correlation to be consistent with other K_C correlations. Since CTOD is simultaneously measured in the J_{IC} test it is included in Table 3 as well.

As discussed earlier, due to the effects of crack tunneling in the interior of the test specimen and the resulting uncracked ligaments near the specimen surface, inaccuracies in crack length determination are introduced which tend to indicate a higher apparent resistance to crack extension than results when side grooving is used to help maintain uniform crack extension. As shown in Figures 8 and 9 and summarized in Table 3, the base metal test (D1) resulted in a J_Q of 130 kJ/m^2 in contrast to 83 kJ/m^2 (D3) when side grooves were introduced. Photographs of both the specimen fracture surfaces are shown in Figure 13 and clearly show the constraining effect of the side grooves and its subsequent effect on maintaining uniform crack extension across the specimen thickness. The dark band adjacent to the fatigue pre-crack is the region of stable crack extension which has been delineated by heat tinting.

The results of weld metal tests shown in Table 3 indicate nearly identical fracture toughness for L-T and T-L oriented test specimens (124 kJ/m^2 and 131 kJ/m^2 Avg. respectively). This is consistent with the CVN tests which also showed nearly identical behavior. In T-L oriented test specimens (Type A) a "pop-in" type of phenomenon was observed in which there was a brief increased rate of load drop during the test. This can be seen in the load-displacement plot for Specimen A2 shown in Figure 10. There was no evidence of change of fracture mode visible on the specimen fracture surface (see Figure 14). This phenomenon may be due to the orientation of the weld metal grain structure in these specimens where the crack front is oriented along single or nearly single columnar grains and may occaisionally advance through these single grains at an increased rate. The columnar grain structure is clearly seen in the fast fracture portion of the fracture surface seen in Figure 14.

The HAZ test results given in Table 3 show that the fracture toughness of the HAZ is similar to the base metal and weld metal as was observed in the CVN tests.

4. DATA ANALYSIS

Although the test data suggests that plane strain conditions will not be satisfied for the thicknesses involved in the double hull structure, the critical stress intensity factors calculated from the CT tests can be used to estimate critical crack sizes for the full scale double hull ship structure. EGW welds are used as longitudinal seams in the ship's hull structure. The primary stress field for hull structure is longitudinal bending which will impose alternating tension and compression forces on the weld seams. For designing ship hulls the American Bureau of Shipping Rules (Part 3 Section 6) limits the primary bending stress to 11.3 L. tons/in.^{2} or 25.38 ksi.

Several types of EGW fabrication flaws were observed to initiate fatigue cracks in the earlier fatigue test program. These flaws ranged from microscopic weld toe flaws and weld surface slag inclusions to clusters of sub-surface porosity. Hydrogen induced cracking was also observed at the fillet at the web-flange intersection. From a fatigue viewpoint the latter two types of flaws were the most severe. Hydrogen induced cracks can be considered the most severe of these types of flaws since they have crack-like acuity and were the largest single flaw observed in the EGW welds. From a fracture viewpoint their severity is compounded in that they reside in the high tensile residual stress field of the weld which can approach yield point magnitudes.

Figure 15 shows the largest hydrogen induced crack observed in a fatigue tested electrogas weld. The depth of the crack is approximately 8 mm (5/16 inch). If we model this crack as a penny shaped crack with a radius of 8 mm as shown in Figure 16 we can estimate the stress intensity, K, for this condition as

$$K = 2/\pi \cdot \sigma \cdot (\pi \cdot a_1)^{1/2} \qquad (1)$$

If we assume the weld flaw resides in a yield point weld residual stress field then $\sigma = \sigma_y = 413$ MPa (60 ksi) and the stress intensity, K, can be calculated as

$$K = 2/\pi \cdot (413 \text{ MPa}) \cdot (\pi \cdot 0.008 \text{ m})^{1/2}$$

$$K = 41.7 \text{ MPa } (\text{m})^{1/2} \qquad (37.9 \text{ ksi } (\text{in})^{1/2})$$

Based upon the results of the fracture toughness tests summarized in Table 3, the static fracture toughness, K_C, of the weld metal can be approximated as 160 MPa $(\text{m})^{1/2}$ (146 ksi$(\text{in})^{1/2}$). From the above calculation it can be seen that the critical stress intensity for instability is approximately 4 times as great as the crack condition existing in the weld. Fracture instability initiating from the most severe of the observed fabrication flaws does not appear to be a concern. A similar calculation can be performed were the crack to grow circularly by fatigue. For the condition shown in Figure 16 where $a_2 = 25.4$ mm, the stress intensity is increased to approximately one-half the critical stress intensity.

For the case of a through-thickness crack condition the critical crack size can be calculated as

$$K_C = \sigma \cdot (\pi \cdot a_c)^{1/2} \qquad (2)$$

where a_c is the half crack length. Using the limiting design stress of 25.38 ksi and the average $K_C = 145$ ksi$(\text{in.})^{1/2}$ measured in the CT tests, the critical crack size for this case is calculated to be 20.8 inches. Leakage of sea water or cargo into the double hull space will occur well before this type of crack reaches a critical size.

5. SUMMARY AND CONCLUSIONS

From the results of this study to determine the fracture toughness characteristics of electrogas welds, the following conclusions can be made:

1. Charpy V-notch tests performed on the base metal (ABS Grade CS), weld metal (AWS EG-82T-G), and HAZ of the electrogas weld indicate a similar level of fracture toughness. The 20 J (15 ft-lb) transition temperature in each case is at least -40 C. Tests performed in the L-T and T-L orientation in the weld metal showed only a small difference in behavior.

2. Based upon the CVN test results fracture of the EGW weld joint can be expected to occur under non-plane strain conditions for static or impact loading at service temperatures as low as -40 C. Under static loading conditions this can be expected at service temperatures as low as -90 C.

3. J_{IC} fracture toughness tests performed on base metal, weld metal, and HAZ of the electrogas weld also show a similar level of fracture toughness in the three regions in all orientations tested. Average J_{IC} values of 120-130 kJ/m^2 were measured in the weld metal and HAZ. Average CTOD values of 0.12-0.15 mm were also measured. Correlating these results to critical stress intensities resulted in average K_C values of 158-165 MPa $(m)^{1/2}$ (144-150 ksi $(in)^{1/2}$).

4. Critical crack lengths were calculated for full-size double hull ships using the fracture toughness test data, a design bending stress, and several crack shapes. Calculations show that shallow surface cracks in the weld region or base metal will not become unstable and through-thickness cracks up to 21 inches in length will remain stable. All of these cracks should be found by visual inspection during periodic tank surveys.

5. The fracture toughness data for the EGW welds confirms that the weld process, electrode and welding procedure that has been developed results in welds with high notch toughness. Any changes in weld wire composition or changes in major welding parameters must be carefully evaluated for its effect on notch toughness.

6. REFERENCES

1. Kaczinski, M.R. and Kaufmann, E.J.
FATIGUE STRENGTH OF ELECTROGAS WELDS IN DOUBLE-HULL CONSTRUCTION, ATLSS Report No. 94-01, Final Report for N00167-93-C-004, Lehigh University, Bethlehem, Pa, January 1994.

2. American Association of State Highway and Transportation Officials
STANDARD SPECIFICATIONS FOR HIGHWAY BRIDGES, 15TH Edition, Washington, D.C., 1992

3. American Welding Society
RECOMMENDED PRACTICES FOR ELECTROGAS WELDING, ASNI/AWS C 5.7-89

4. American Welding Society
SPECIFICATION FOR CARBON AND LOW-ALLOY STEEL ELECTRODES FOR ELECTROGAS WELDING, ASNI/AWS A 5.26-91

5. American Society for Testing and Materials
ASTM E-813-89
Standard Test Method for J_{IC}, A Measure of Fracture Toughness

6. Wellman, G.W., Rolfe, S.T.
"Engineering Aspects of CTOD Fracture Toughness Testing"
WRC Bulletin 299, Nov. 1984.

7. TABLES

Specimen Code	Specimen Type	B, Thickness mm (in)	W, Width mm (in)	a_f/W
A1	WM, T-L	24.49 (0.964)	50.80 (2.000)	0.60
A2	WM, T-L	24.49 (0.964)	50.77 (1.999)	0.60
A3	WM, T-L	24.54 (0.966)	50.80 (2.000)	0.60
B1	HAZ, T-L	24.71 (0.973)	50.80 (2.000)	0.55
B2	HAZ, T-L	24.69 (0.972)	50.80 (2.000)	0.55
B3	HAZ, T-L	24.69 (0.972)	50.77 (1.999)	0.55
C1	WM, L-T	24.49 (0.964)	50.77 (1.999)	0.60
C2	WM, L-T	24.46 (0.963)	50.80 (2.000)	0.60
C3	WM, L-T	24.49 (0.964)	50.77 (1.999)	0.60
D1	BM, T-L	24.71 (0.973)	50.80 (2.000)	0.60
D2	BM, T-L	24.71 (0.973)	50.77 (1.999)	0.60
D3	BM, T-L	24.74 (0.974)	50.77 (1.999)	0.60

Table 1 - CT Specimen Dimensions

Temperature °C	Weld Metal T-L Joules (ft-lbs)	Weld Metal L-T Joules (ft-lbs)	Base Metal T-L Joules (ft-lbs)	HAZ T-L Joules (ft-lbs)
-80	14.2 (10.5)	17.0 (12.5)		
-80	13.6 (10.0)	10.8 (8.0)		
-80	16.3 (12.0)	10.8 (8.0)		
-60	29.8 (22.0)	36.6 (27.0)	4.1 (3.0)	13.6 (10.0)
-60	30.5 (22.5)	22.4 (16.5)	8.1 (6.0)	14.2 (10.5)
-60	31.2 (23.0)	22.1 (18.5)	11.5 (8.5)	24.4 (18.0)
-40	35.9 (26.5)	64.4 (47.5)	10.8 (8.0)	21.7 (16.0)
-40	42.7 (31.5)	52.9 (39.0)	28.5 (21.0)	21.7 (16.0)
-40	50.2 (37.0)	50.9 (37.5)	31.2 (23.0)	21.7 (16.0)
0	99.7 (73.5)	84.8 (62.5)	50.2 (37.0)	29.8 (22.0)
0	101.7 (75.0)	84.8 (62.5)	57.0 (42.0)	40.7 (30.0)
0	120.0 (88.5)	73.2 (54.0)	67.8 (50.0)	42.0 (31.0)
24.5	119.3 (88.0)	86.8 (64.0)	70.5 (52.0)	47.5 (35.0)*
24.5	127.5 (94.0)	111.2 (82.0)	80.0 (59.0)	61.0 (45.0)*
24.5	137.6 (101.5)	117.3 (86.5)	83.4 (61.5)	71.9 (53.0)*
50	122.0 (90.0)	105.8 (78.0)	110.5 (81.5)	75.9 (56.0)
50	126.8 (93.5)	113.9 (84.0)	118.7 (87.5)	81.4 (60.0)
50	135.6 (100.0)	166.1 (122.5)	120.7 (89.0)	109.2 (80.5)
70			116.6 (86.0)	86.8 (64.0)
70			118.0 (87.0)	97.6 (72.0)
70			122.7 (90.5)	

* Test temperature 20°C

Table 2 - Charpy V-Notch Test Results

Specimen Code	Specimen Type	J_Q (E813-87) kJ/m^2 (in-lb/in^2)	$K_Q=(J_QE)^{1/2}$ MPa(m)$^{1/2}$ (ksi(in)$^{1/2}$)	CTOD δ_c mm (in)
A1	WM, T-L	146 (834)	174 (158)	0.14 (0.0055)
A2	WM, T-L	123 (700)	159 (145)	0.13 (0.0051)
A3	WM, T-L	125 (712)	160 (146)	0.13 (0.0050)
Average		131 (749)	165 (150)	0.13 (0.0052)
B1	HAZ, T-L	137 (782)	168 (153)	0.17 (0.0067)
B2	HAZ, T-L	106 (608)	148 (135)	0.13 (0.0050)
B3	HAZ, T-L	120 (688)	158 (144)	0.15 (0.0061)
Average		121 (692)	158 (144)	0.15 (0.0059)
C1	WM, L-T	140 (800)	170 (155)	0.14 (0.0055)
C2	WM, L-T	121 (688)	158 (144)	0.13 (0.0051)
C3	WM, L-T	114 (651)	154 (140)	0.10 (0.0038)
Average		124 (713)	160 (146)	0.12 (0.0048)
D1*	BM, T-L	130 (746)	165 (150)	0.26 (0.0103)
D3	BM, T-L	83 (475)	131 (119)	0.09 (0.0037)

* Without side-grooves

Table 3 - J_{IC} Fracture Toughness Test Results

8. FIGURES

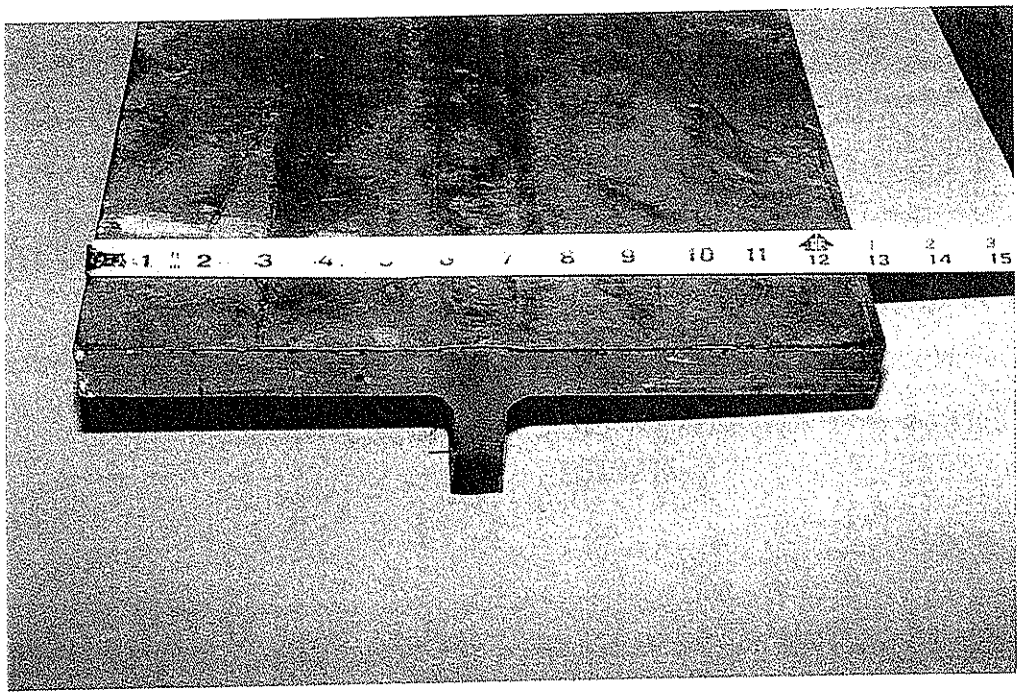

Figure 1 End view of EGW test panel [3/94/15-12]

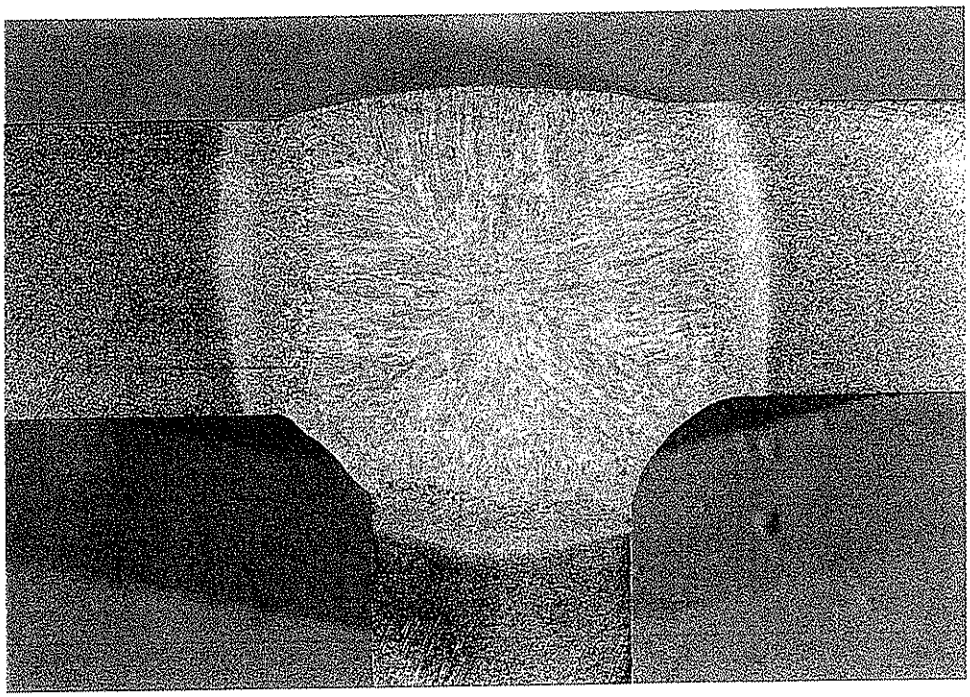

Figure 2 Etched cross-section of electrogas weld. [6/94/20-6]

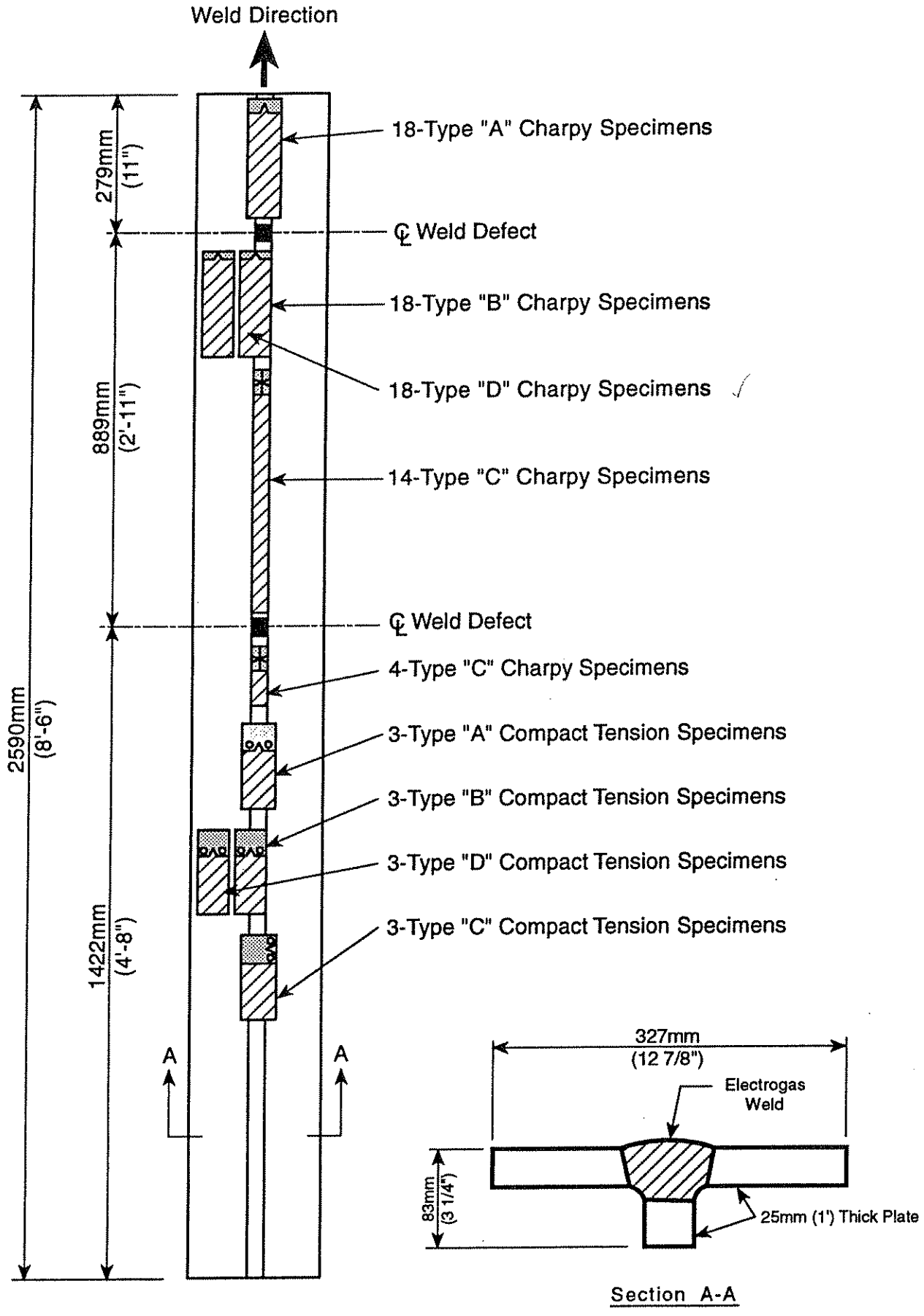

Figure 3 Test Specimen Layout

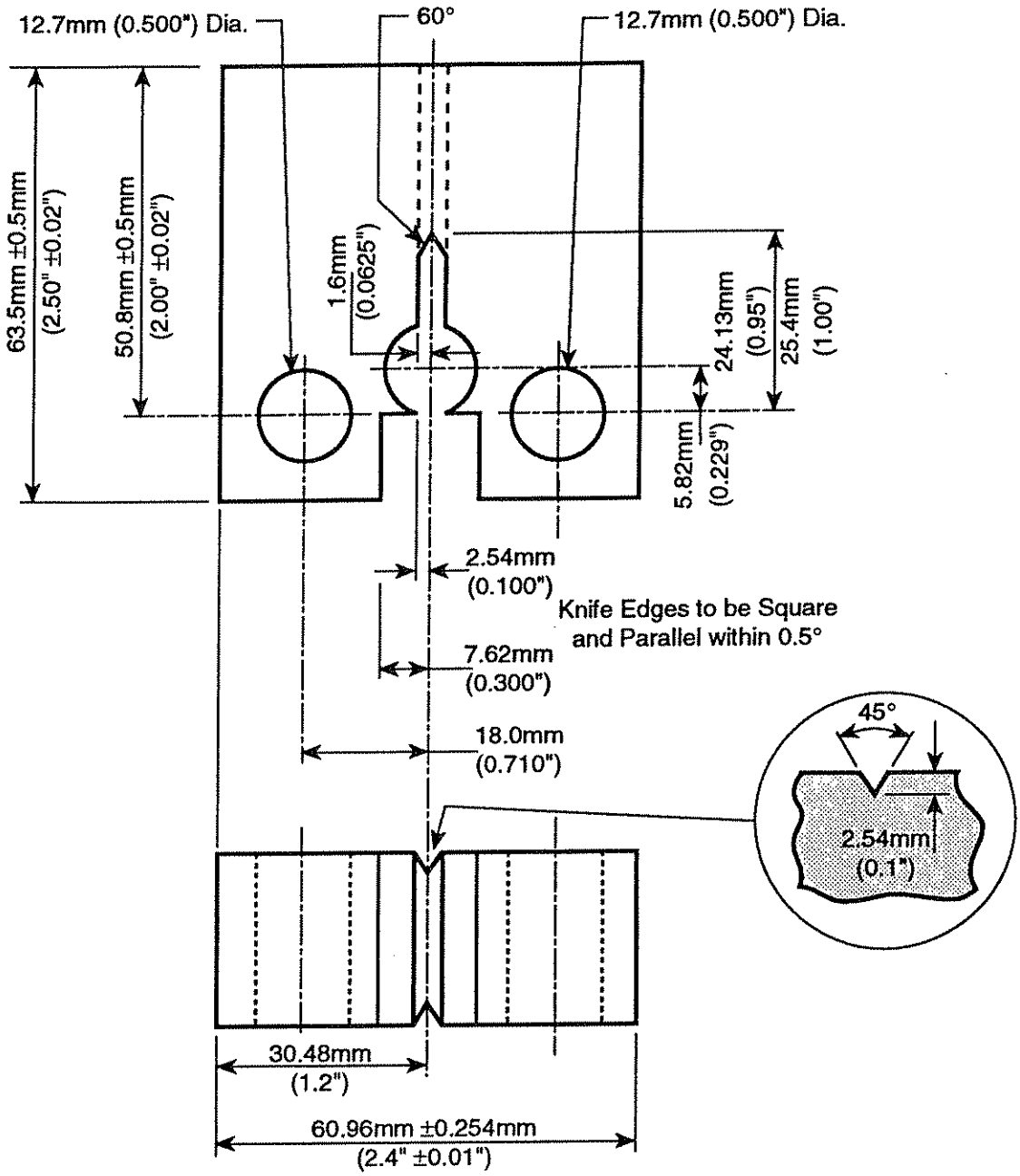

Figure 4 Compact Tension (CT) Specimen Dimensions

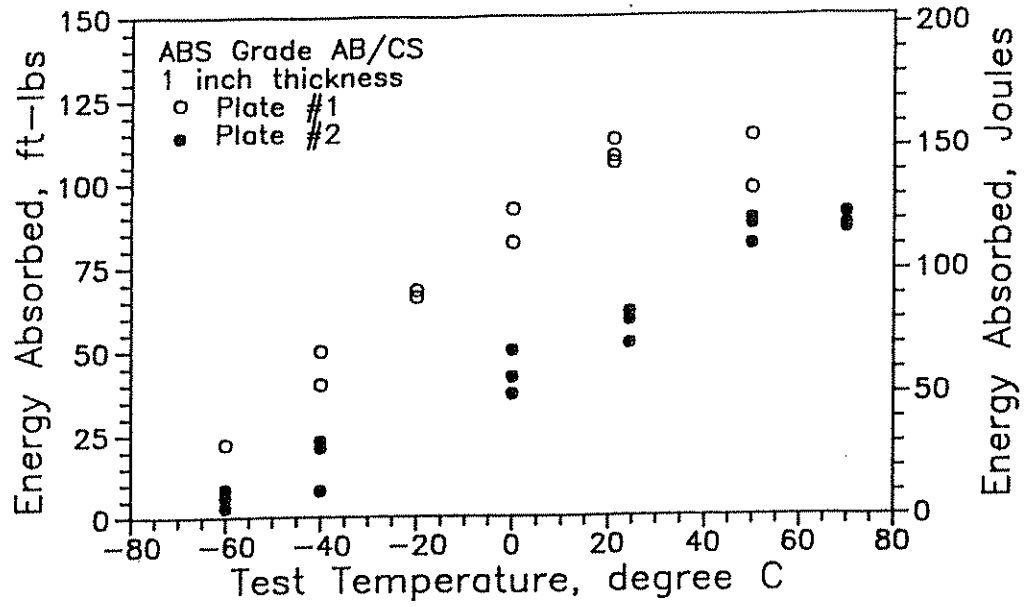

Figure 5 Base Metal Charpy V-Notch Test Results.
Plate #2 data is from the plate used in the present study.
Plate #1 data is from the previous fatigue study.

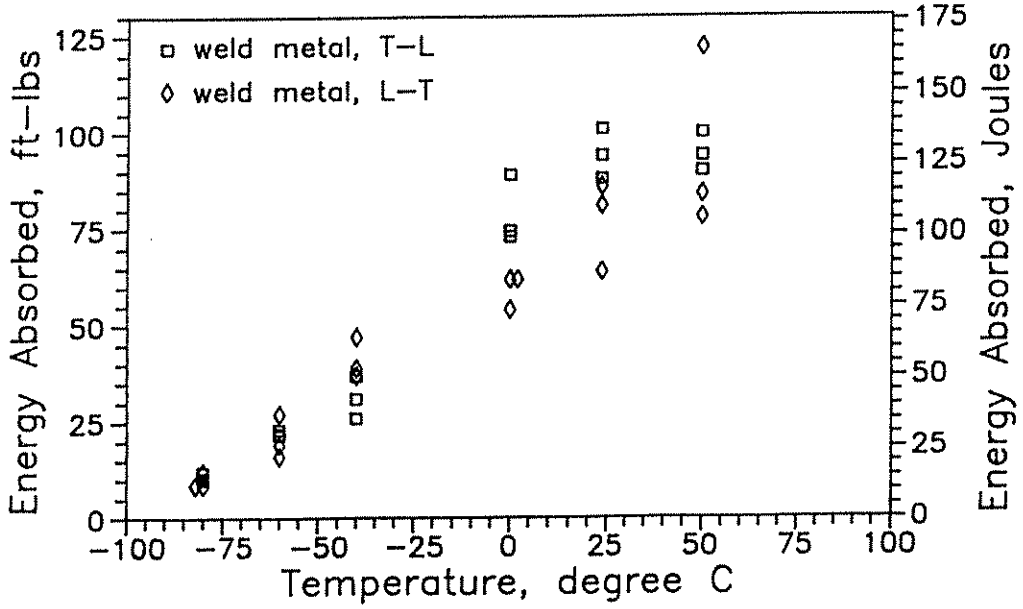

Figure 6 Electrogas weld metal Charpy V-Notch test results.

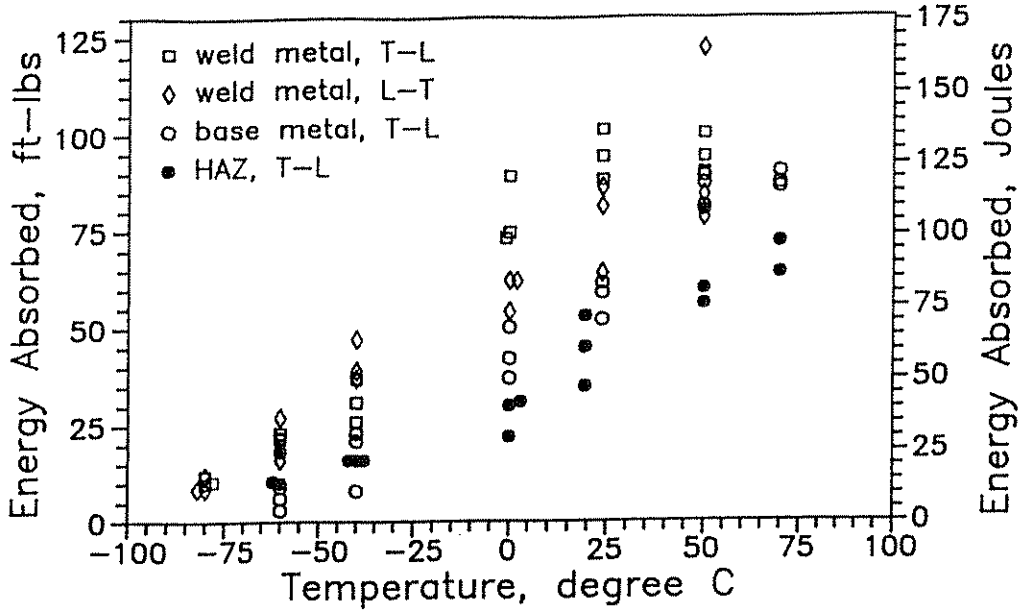

Figure 7 Charpy V-Notch Test Results for Base Metal, Weld Metal, and HAZ.

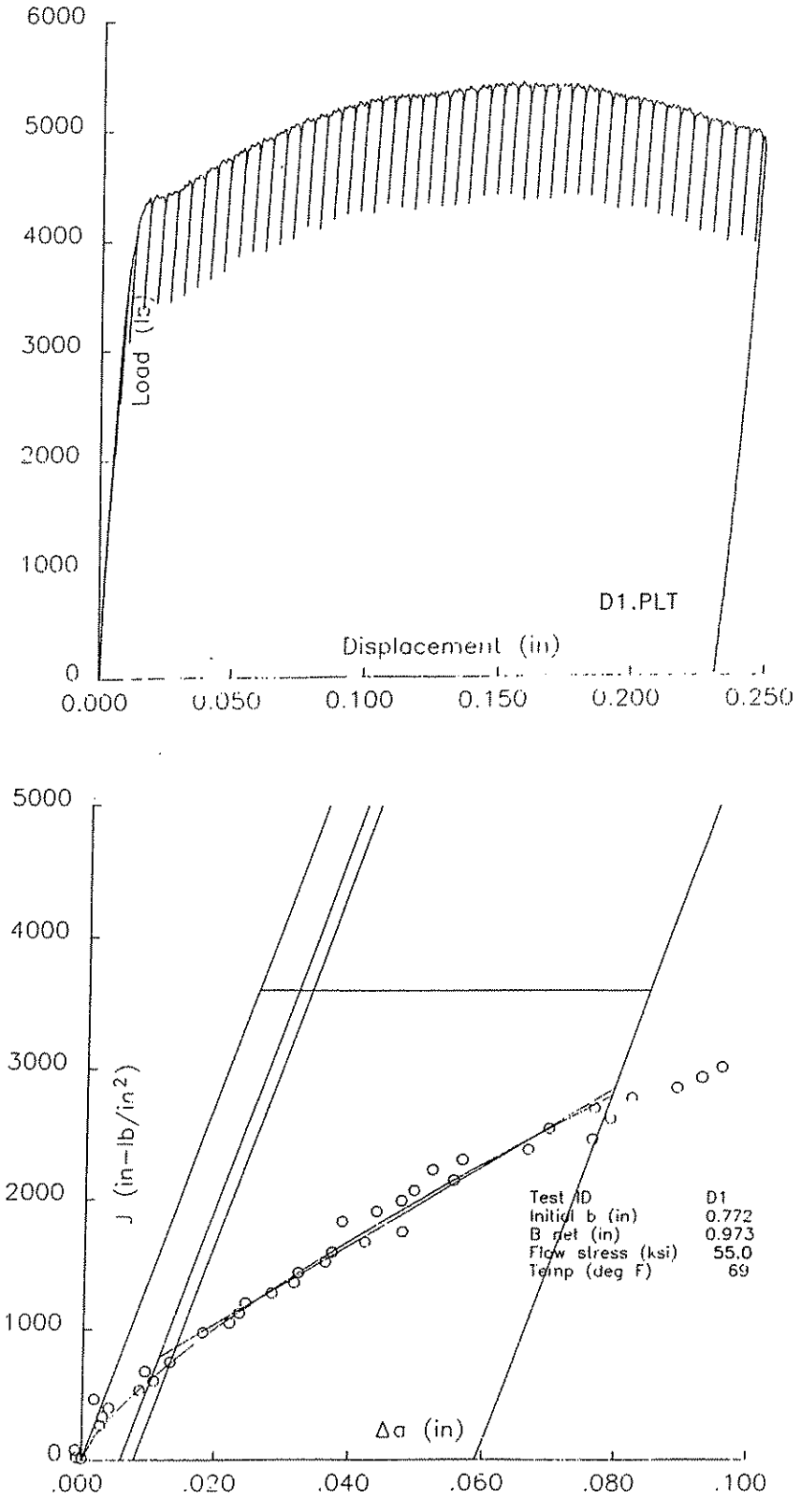

Figure 8 Load-Displacement and J-Δa plots for Specimen D1.

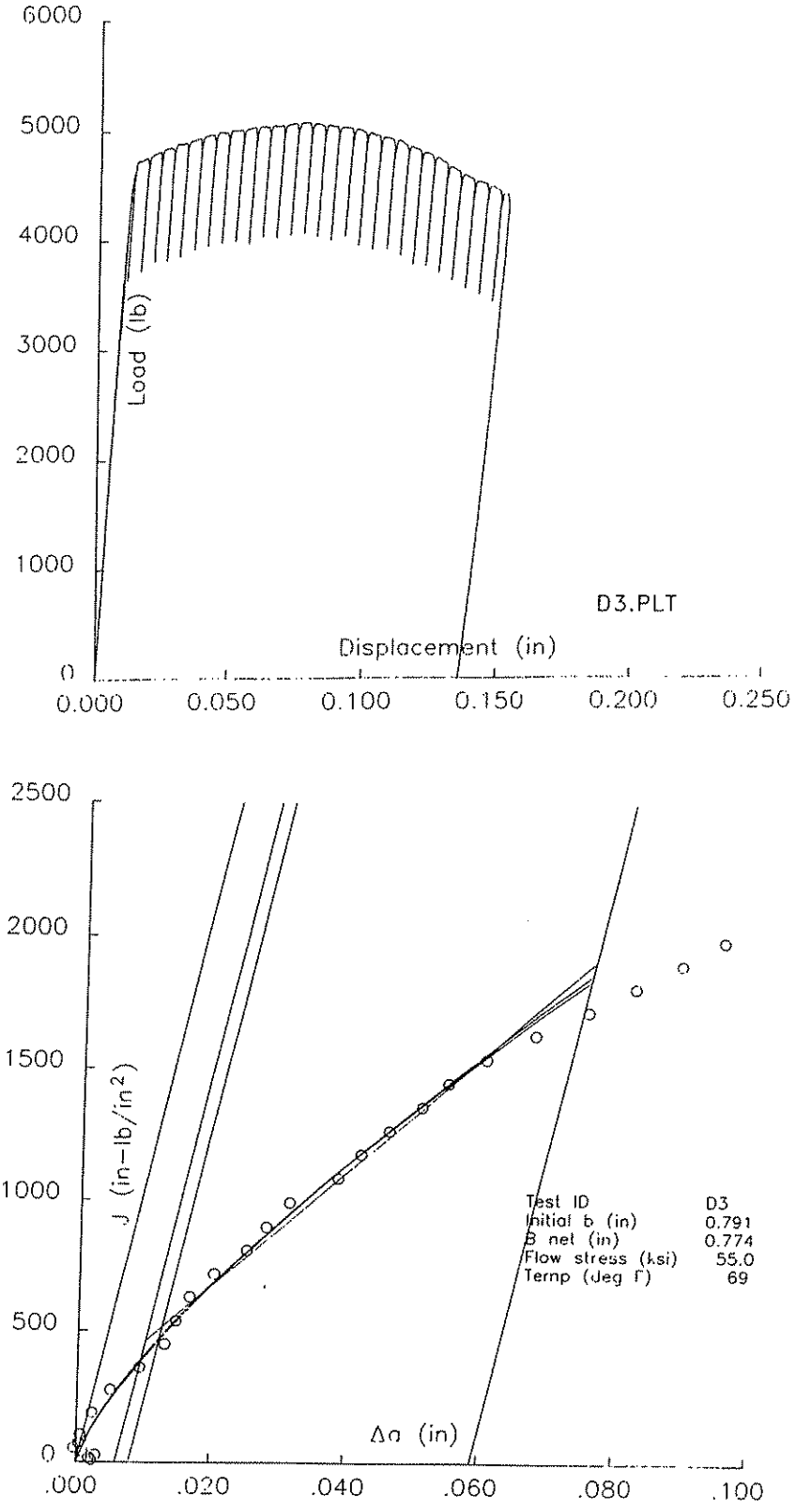

Figure 9 Load-Displacement and J-Δa Plots For Specimen D3.

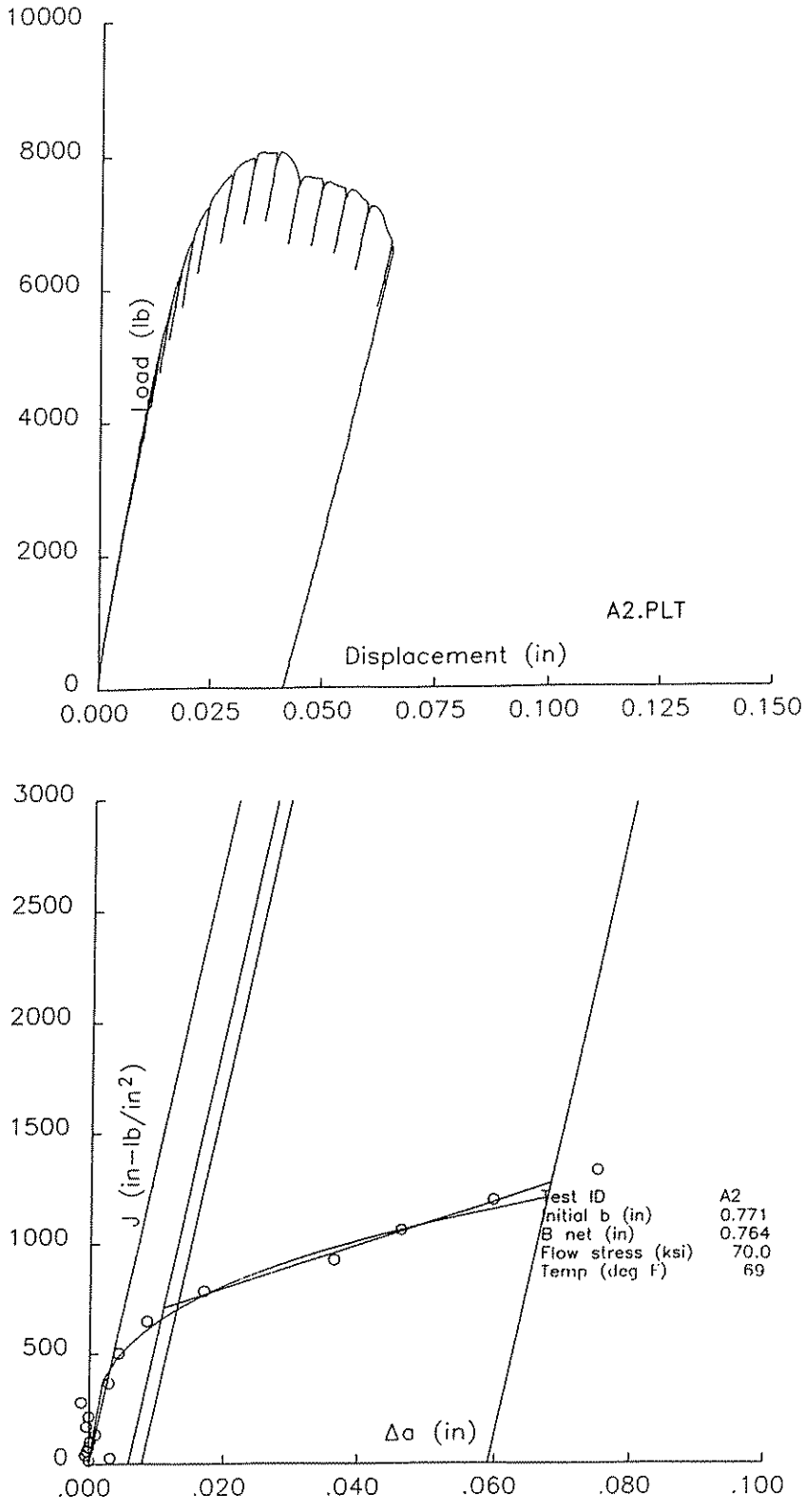

Figure 10 Load-Displacement and J-Δa Plots for Specimen A2.

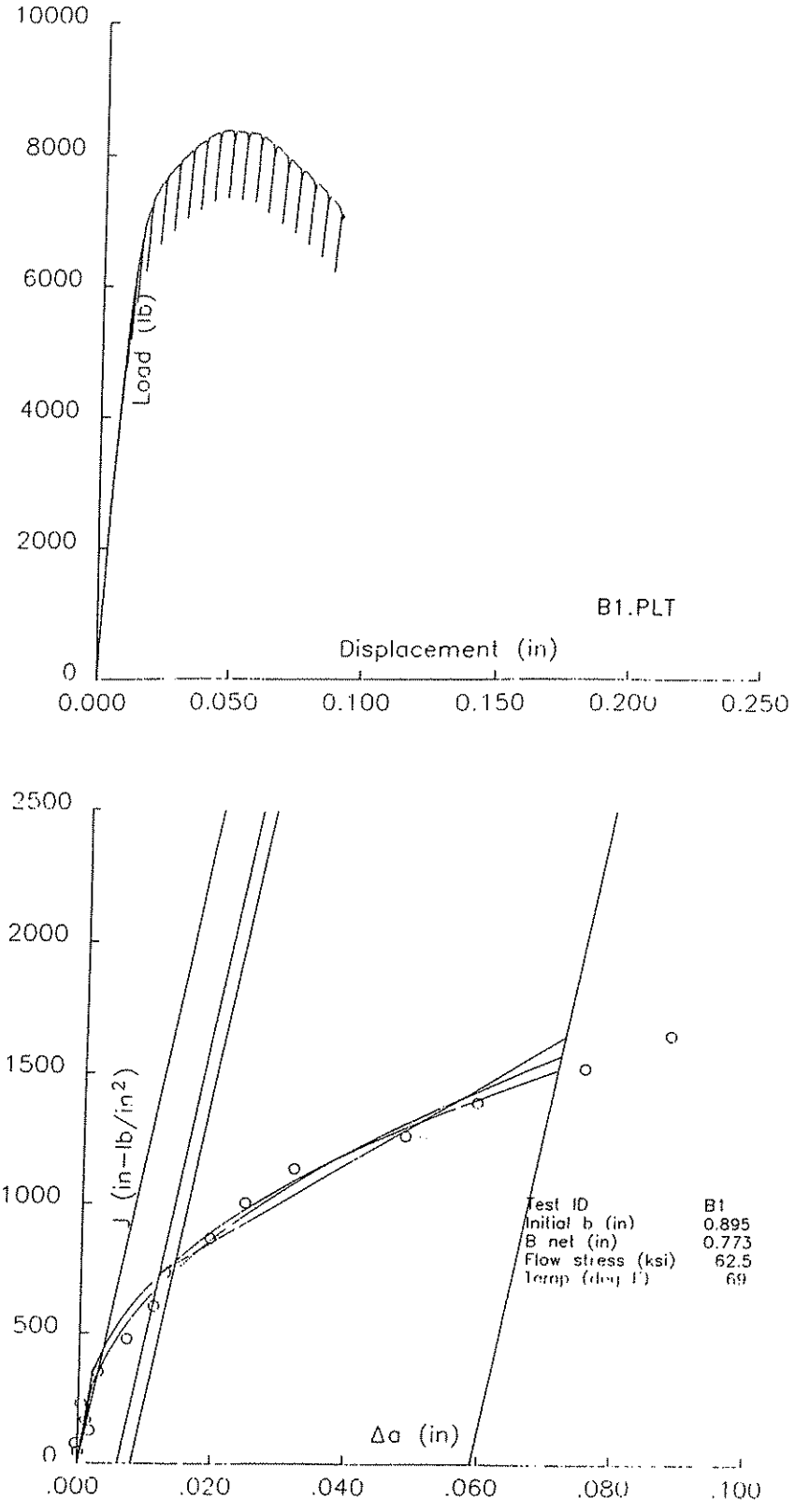

Figure 11 Load-Displacement and J-Δa Plots for Specimen B1.

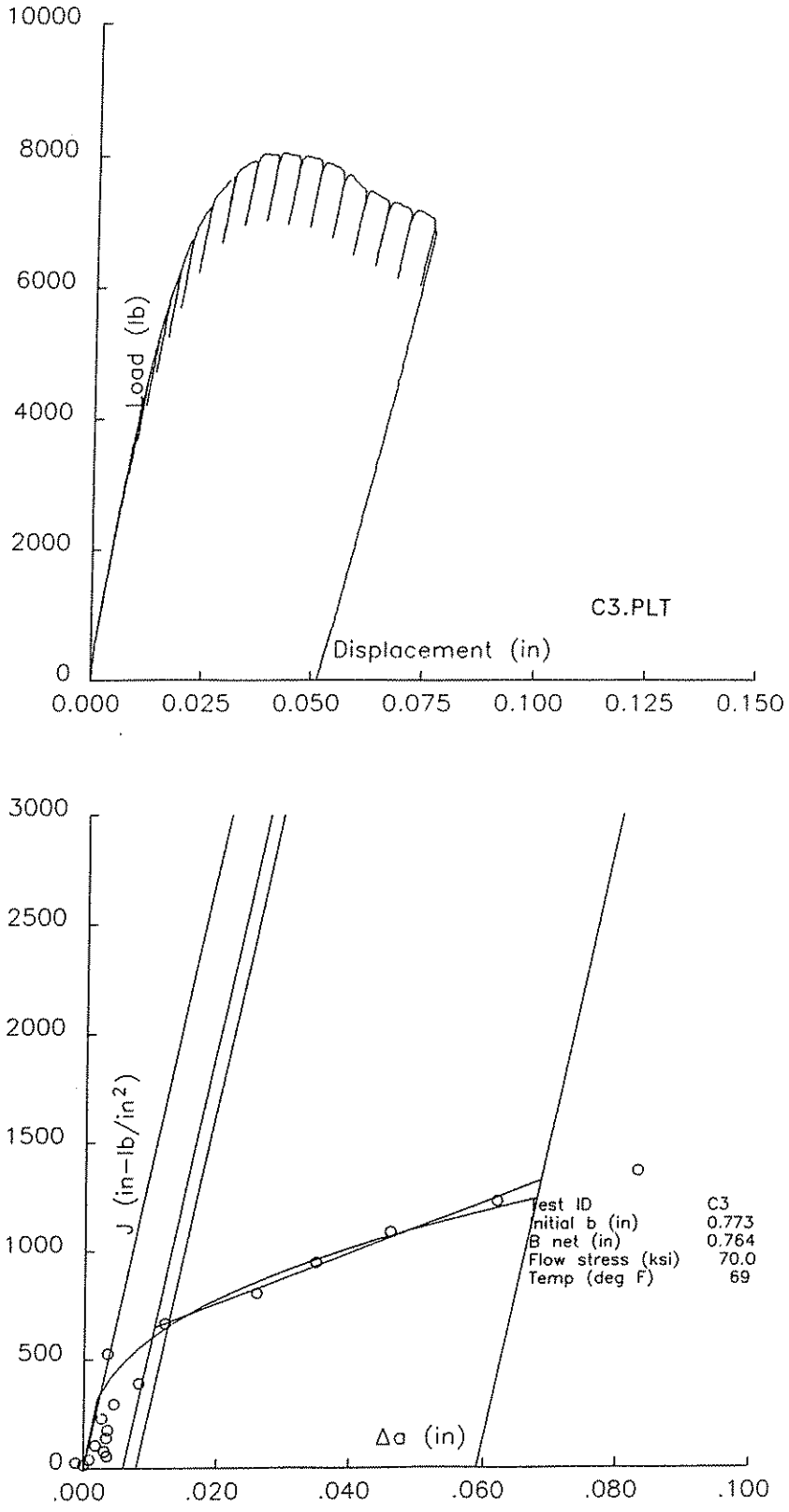

Figure 12 Load-Displacement and J-Δa Plots For Specimen C3.

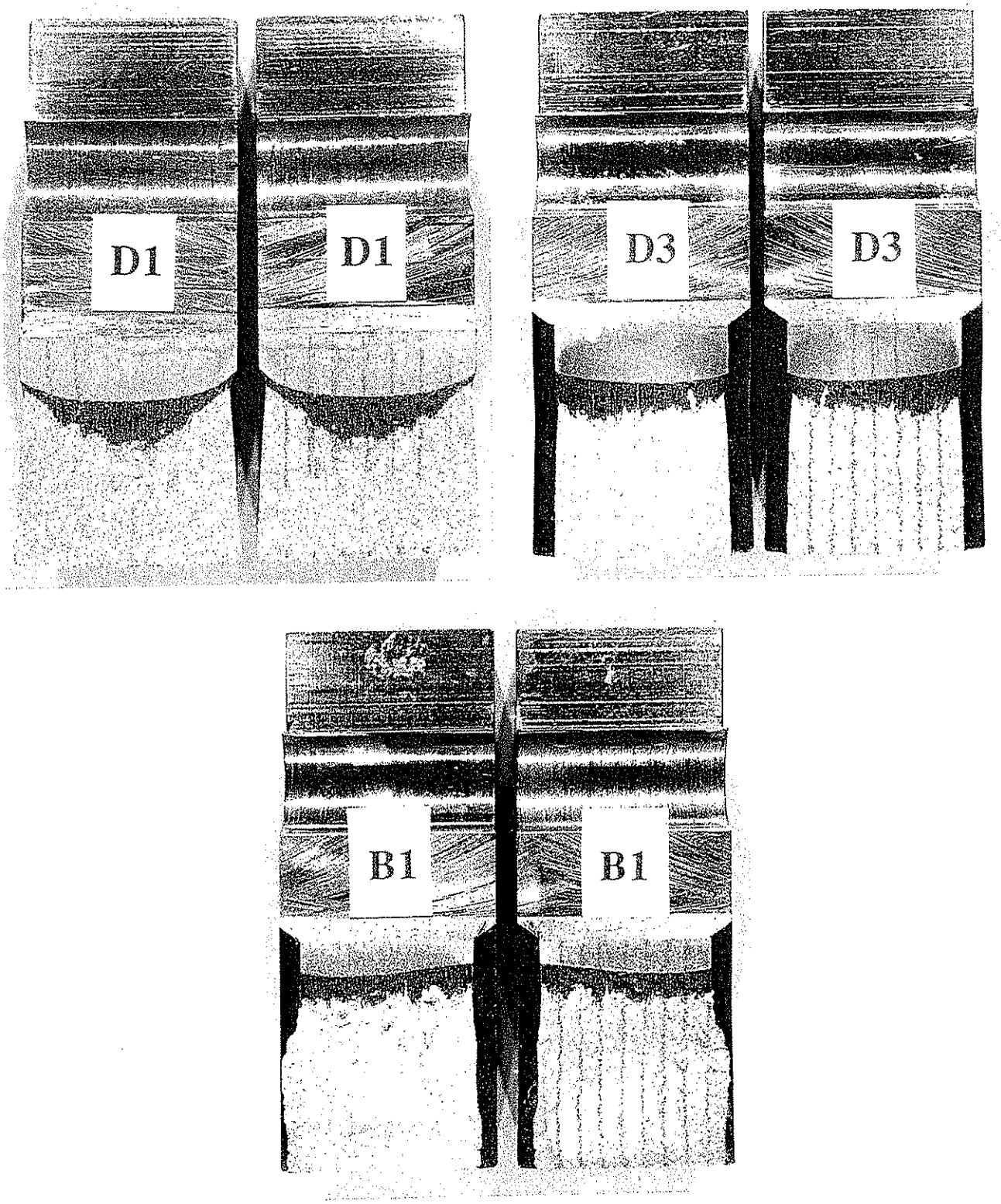

Figure 13 Typical CT Specimen Fracture Surfaces.
Top) Base metal [6/94/1-9,6/94/1-11]
Bottom) HAZ [6/94/1-5]

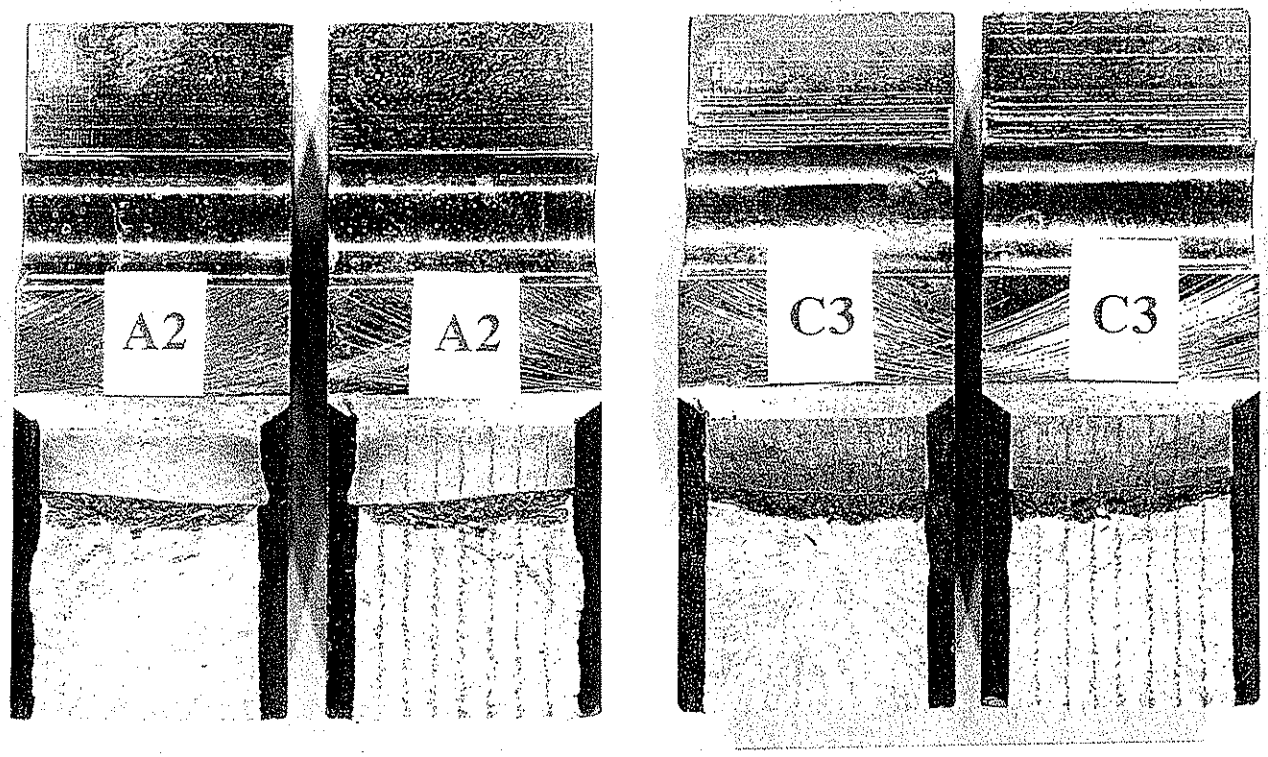

Figure 14 Typical Weld Metal CT Specimen Fracture Surface
[6/94/1-3, 6/94/1-7]

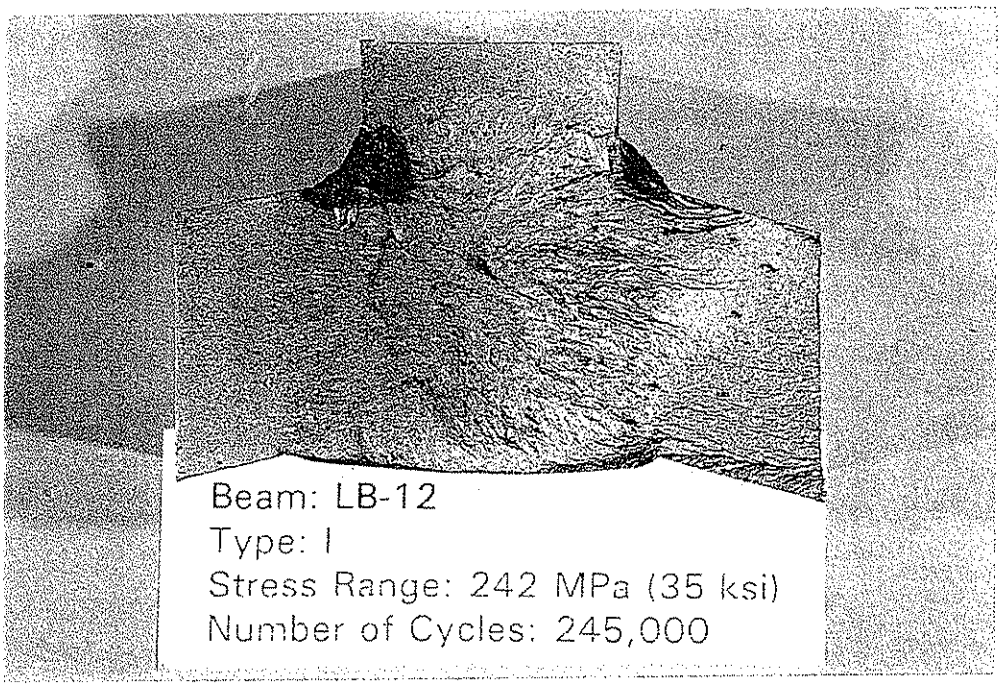

Figure 15 Hydrogen induced weld metal crack observed on EGW fatigue fracture surface. [12/93/3-8]

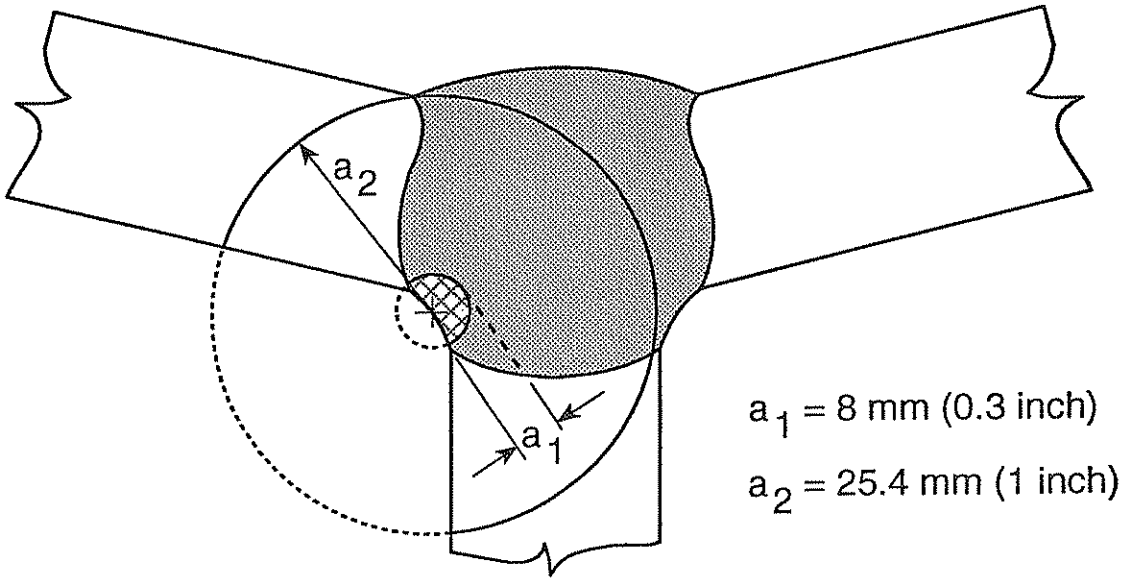

Figure 16 Crack model for EGW weld detail.